CHALMERS

On Indoor Positioning for Mobile Devices

Master's Thesis in Communication Engineering &
Master's Thesis in Integrated Electronic Systems Design

PABLO ESTEBAN QUIROGA GARCIA
WENJIE LI

Department of Signals and Systems
CHALMERS UNIVERSITY OF TECHNOLOGY
Göteborg, Sverige, 2011
Master's Thesis EX049/2011

Abstract

Pedestrian Navigation Systems (PNS) have gained popularity for their potential application to track people in risky environments or in rescue missions. Studies have been done to integrate information from accelerometers, gyroscopes, magnetometers, barometers, and GPS to accurately track the location of subjects on indoor and outdoor environments.

In this thesis, accelerometers, gyroscopes, and magnetometers were installed on a mobile phone to track the position of a person indoors without the aid of wireless technologies. The phone was placed on the waist and the front pockets of the pants of the users. To determine the travelled distance, a single vertical accelerometer was used. Also, a simple sensor fusion algorithm based on the Kalman filter was designed to determine the heading of the person using information from the gyroscope and magnetometers.

Experiments were conducted on different scenarios and the results indicate that the typical positioning accuracy is below 5% for distances up to 170 meters. Issues and proposed improvements to the system are also discussed in this work.

Keywords: Sensor Fusion, Pedestrian Navigation Systems, Kalman filter, step detection, step length, heading determination, disturbance detector.

Acknowledgements

A couple of weeks ago, I was walking with Wenjie and this guy -which I will call *Emil* for anonymity. Emil was talking about the importance of the order in which you acknowledge people in your thesis. Considering that I have (in alphabetical order) bosses, co-workers, family, friends, and sponsors, that leaves me in a difficult spot. This is why I have decided to thank Emil first and last. That way, everybody can rest assured that I appreciate them and that the order I wrote the acknowledgements does not really matter.

To those that made this dream possible. To STINT and ITESM, but specially to *la* Dra. Laura and Katarina. Thank you for believing in me.

To my family in Sweden and Europe. Maru, Fredrik, Michelle, Susana and Chano. Annie, Christian, Cécilia, Marion and the Nottebaert-Totis families. Alberto, Andy, Jorge, Fernando, Matt, Oana, Sumaiya, Olga, Pina, Marieke, Pol, Sylvain, Emilie, Laleh, Abhi, Saimir, Caro, Alavi, Fidel, Fra, Camilo, Irfan, Simon, and Isa. For making me feel supported these two years and for making of this a magnific experience.

To everybody directly involved in this thesis work. To ASCOM for chosing me to work in this project, but specially to our supervisor Carl-Johan for providing ideas and feedback all the time. To the "lunch gang" for making every day at work a nice day. To our examiner Lennart, for opening our eyes when we could not see further and for being a cool examiner and advisor. To Wenjie, for being committed to this work, and for being stubborn as well... ‿ you made me better!

Al Guillermo, por *invertirle* tanto -y 'pa que no diga que no le doy su espacio.

A mi Padre, a mi Madre, a José y a David. A Gloria y a mi abuela Virginia. A toda mi familia de nacimiento y extendida por voluntad. Por ser la base sobre la cual mi vida se ha construido y se sigue construyendo. Por los momentos felices y difíciles. Por todo.

Quiero dedicar este trabajo a mi sobrina Elena. Por que siga sonriendo como la veo sonreir aun estando lejos.

Ah yes, and thank you, Emil.

<div align="right">Pablo Esteban Quiroga Garcia, Göteborg, Sverige.</div>

Acknowledgements

I would like to express my sincere gratitude to everyone who helped and supported me during this 20 weeks of thesis work on 'Indoor Positioning for Mobile Devices'. First of all, thank to ASCOM Sweden AB for offering me such an interesting and practical topic. I really enjoyed and learned a lot during my time in ASCOM.

Foremost I would like to express my gratitude to our supervisor Carl-Johan Helgesson, for his guidance and support throughout the stages of my work. He always gave me very good suggestions when something *blocked* my way. He helped me to have better understanding of different problem solving methods and to think deeply and comprehensively. I am impressed by his humor and kindness.

I would also like to thank to our examiner Lennart Svensson. He always explained me the theory in a very simple and impressive way; it was quite helpful for my thesis work. I always learned a lot during our fruitful discussions. I also appreciate that he could have very good balance between academic research and colorful life.

Thanks to all the talented engineers in the hardware section at ASCOM for giving me your support, especially Thomas Harju, the nice and kind leader of this team; Irfan, young and promising hardware engineer, and we also became friends during the time here; Mikael, I really appreciate his hard working, and he is really a person who was born to be an engineer and could use technical things everywhere. I will also like to give my deep gratitude to my friends: Andreas, Emil, Simon, Jose, and Claudia, for making my thesis work here more colorful and interesting.

Special thanks to my dear partner of this thesis work, Pablo, who I met because of this project. We shared our happiness and disappointments along with our thesis project and our life during these 5 months. We had good cooperation during this time. I am glad to have such a funny and intellectual friend, I also learned a lot from him. Don't forget, I want to be the Chinese teacher of your 'spy' son!

I also want to thank to all my friends in Göteborg. Thanks for your support, share, and company. I never felt lonely during my time in Sweden, far from my home.

Finally, I want to express my deepest gratitude to my parents who are always supporting me no matter what I want and no matter what I have done. Thank you for your unconditional love and trust to me. Even though you are 8000km away, you are always here in my heart.

<div align="right">Wenjie Li, Göteborg, Sverige.</div>

Contents

Chapter 1

Introduction

Inertial Navigation Systems (INS) were born from the need to track the movement of objects using accelerometers and gyroscopes. As many other research studies, the military pioneered in the field to control gun-fire systems, rockets, and aircrafts [1].With the evolution to Micro-Electro-Mechanical Systems (MEMS), sensor size and cost have enabled applications in other fields, for instance, car navigation.

Pedestrian Navigation Systems (PNS) have increased in popularity among researchers. PNS are formed by inertial sensors, magnetometers, barometers, temperature sensors, and even GPS. Researchers on the field have worked on different techniques to solve the tracking problem by putting the sensors in different places of the subject [9] [6]. The purpose, motivation, and scope of this work are mentioned next.

The research performed by the authors is presented on chapter 2. Then, the implementation of the system is mentioned in detail on chapter 3. The experiments, results, and issues are discussed on chapter 4. An last, the conclusion and proposed further work are presented on chapter 5.

1.1 Purpose and Motivation

This master's thesis was made in collaboration with ASCOM Wireless Solutions. ASCOM strive to deliver solutions for wireless on-site communications to support and optimize their customers' mission. This is achieved through purpose-built handsets, wireless voice and message transmission systems, and customized alarm and positioning applications. The current positioning applications rely on wireless short range beacons that help to identify when a user has crossed a certain place in a building. This master's thesis focuses on how to improve the existing positioning application by using inertial and magnetic sensors.

Enhancements on this application could give better knowledge of the current position of the person, which could be vital in rescue missions or to locate workers in risky environments, for instance, guards in correctional facilities. Also, this could help to reduce the equipment to be installed in the buildings, helping to reduce costs and to make the positioning solution more flexible.

The purpose of this work is to make a working demo for a sensor-based indoor positioning solution and to display the results in a map. Figure 1.1 shows an example of a desired result.

1.2 Scope

As this work represents the start of a new project, restrictions had to be made in order to measure the advance and to identify the areas to improve. Accelerometers, magnetometers, and a single gyroscope were the only sensors used in this work. The position of the mobile phone was restricted to the pocket and waist of the user, and the starting location and heading were considered to be known. Still, different persons walking at their own natural pace were used to test the system in different environments.

1.3 Method

The accelerometer in the vertical axis was used to find the number of steps given by the user as well as to calculate the length of each one of them. The magnetometers
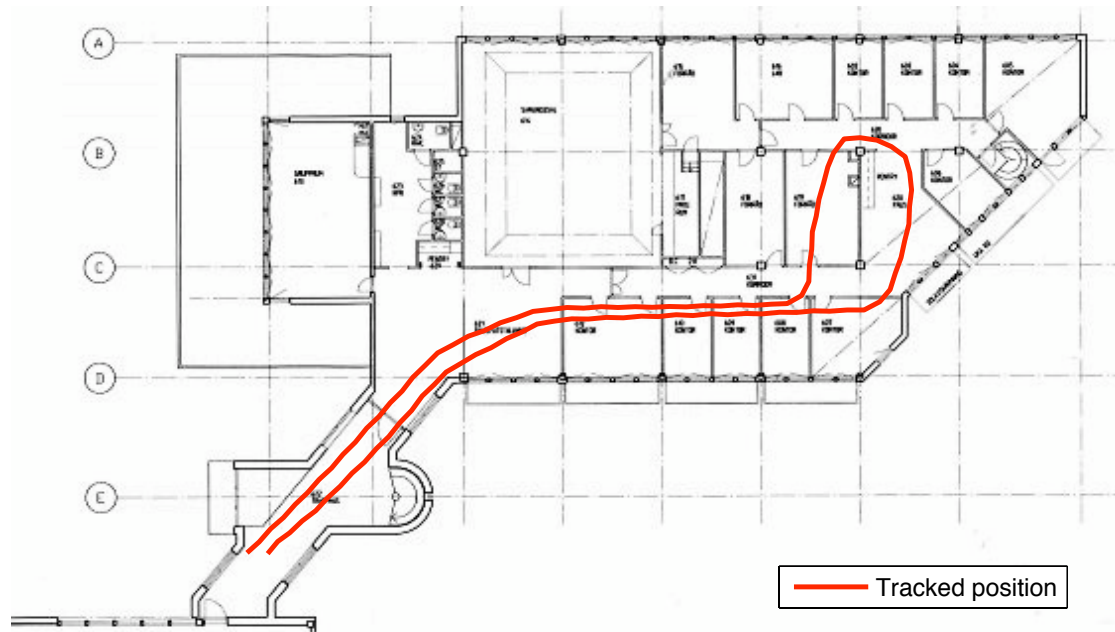
Figure 1.1: Example of results obtained with the positioning demo.

were used to find the heading and the tilt of the module was calibrated with the aid of the 3-axis accelerometer. Also, a Kalman filter was used to fusion the gyroscope angular rate and the compass heading with a disturbance detector. Finally, the length and heading per step were plotted in a map and the results were obtained.

Chapter 2

Background

DIFFERENT STRATEGIES have been used by researchers to accurately track the position of an object while its moving. This chapter briefly reviews some of the most relevant studies made in the field of PNS. The distance and heading estimation algorithms are mentioned as well as the basic calibration needed for operation. Also, methods to detect magnetic disturbances are explained and finally, an introduction to the Kalman filters is given with examples of how other authors have contributed to the field.

2.1   Distance

Different algorithms have been proposed to calculate the distance a person has walked. If an accelerometer is available, the first solution that one might think of is to integrate twice the acceleration to obtain the total distance. The problem with this approach is that sensors are inexact and their errors would accumulate by integrating. To avoid this, researchers have come up with methods to detect steps and estimate their lengths without integrating the acceleration.

2.1.1 Step Detection

There are several ways to do step detection using accelerometer information, but the main difference strives on whether the sensor is located on the foot, waist, or in a different place. Since this project deals with positioning using a mobile device, the sensors are assumed to be on the waist or the pocket and not on the feet. An example of how an accelerometer signal looks like is shown in figure 2.1.
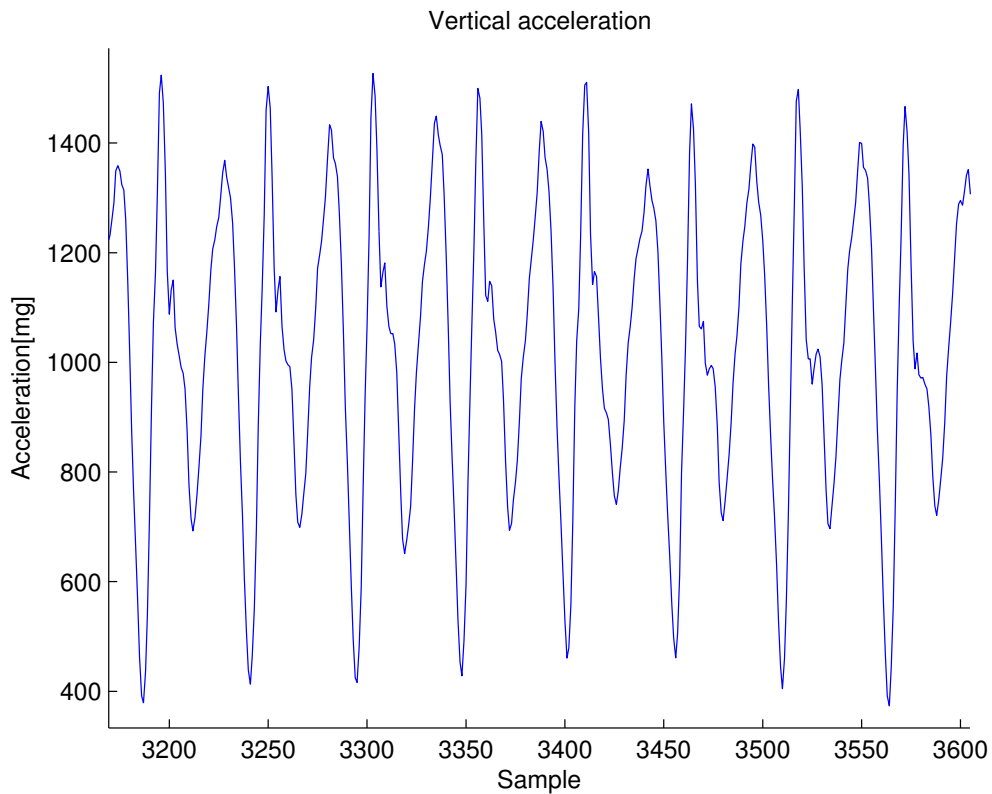

Figure 2.1: Vertical acceleration signal of a person walking.

A popular method proposed by Weinberg [3] detects the peaks on the measurements by using a single accelerometer to sense the vertical acceleration. On the other hand, Käppi [2] uses the norm of a triad accelerometer to find where the signal crosses the zero reference within a recognition window.

2.1.2   Step Length

Regarding step length estimation, Käppi [2] states that it is possible to obtain an estimate comparable to the walked distance by integrating the absolute value of the acceleration magnitude of each step. Weinberg [3] instead, proposed a nonlinear method that uses the maximum and minimum peaks obtained during the step detection phase, and a constant that can be fixed or adjusted for different users or type of activity, such as walking or running. This method is given by

$$L_{\text{step}} = k \cdot \sqrt[4]{A_{\max} - A_{\min}}, \tag{2.1}$$

where L_{step} stands for the step length, $A_{\max}$ and $A_{\min}$ are the maximum and minimum *vertical* acceleration values within the step, and k the adjustable constant mentioned before.

Shin [5] proposed an adaptive method known as the linear method

$$L_{\text{step}} = a \cdot f + b \cdot v + c. \tag{2.2}$$

In this method, the distance is estimated by calculating the walking frequency (f) and acceleration variance (v) and scaling the results using the constants a, b, c that can be calculated during a training stage using linear regression.

2.2   Heading

To successfully track the movement indoors, it is crucial to find an accurate representation of the direction the person is moving towards. This direction is known as the *heading*. In the next sections, the principles to find the heading using magnetometers and gyroscopes is discussed.
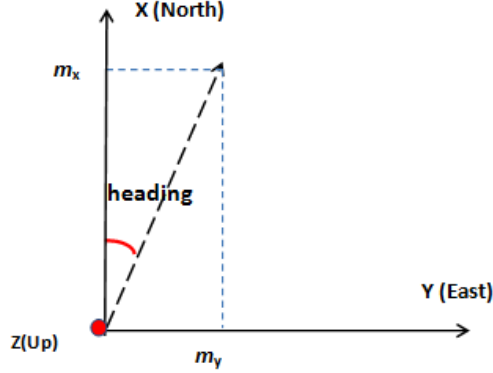
Figure 2.2: The heading is referenced to the north and is found using the magnetic readings in X and Y axes.

2.2.1 Principles

To find the heading using magnetometers, it is only necessary to know the horizontal magnetic components of the Earth. This can be achieved by using the equation,

$$h = \arctan\left(\frac{m_y}{m_x}\right), \tag{2.3}$$

where h stands for the heading and m_x, m_y are the magnetic readings in the x and y axis, respectively. See figure 2.2. It is important to mention that the compass indicates the heading referenced to the magnetic north. To correct the heading to the geographic north, the angle between the magnetic north and the true north must be compensated [8].

It is important to note that the compass can be easily corrupted by other surrounding magnetic fields. Chen [6] mentions that compasses can be corrupted by *predictable* and *unpredictable* errors. Predictable errors come from sources such as hard and soft iron effects, tilt of the phone, and magnetic declination. In sections 2.2.3 and 2.2.4, the basic compass calibration to deal with these types of errors is discussed.

Unpredictable or *dynamic* errors can be caused by objects like computers, phones, calculators, and even metallic tables and chairs. The errors cannot be removed

from the heading information but their effect on the system can be reduced using different techniques. Section 2.3 presents ideas proposed by Käppi [2], Kim [9], and Laddeto [7].

To determine the heading using gyroscope information only, it is necessary to integrate the angular rate over the period of time where the person is walking. It is important to notice that the initial heading must be known, since the gyroscope only knows about the turns the person has made or their relative position. The initial heading can be supplied to the gyroscope using the compass heading or with a positioning beacon.

Gyroscopes and magnetometers are constituted differently and therefore, have different strengths and weaknesses. The angular rate of the gyroscope is generated by an electro-mechanical oscillating mass that is sourceless and relatively immune to environmental disturbances [4]. Gyroscopes have good performance on quick turns but are subject to bias drifts. When the bias drift is integrated, it results in an increment of the error magnitude at every instance. On the other hand, the compass does not suffer from bias drifts but has a slow response to quick turns and can be easily corrupted by surrounding magnetic disturbances [9]. Sections 2.3 and 2.4 introduce how to combine the gyroscopes and magnetometers to take advantage of their strengths and compensate for their weaknesses.

2.2.2 Reference Frames

Reference frames have to be defined in order to get the right heading. The main reference frame is called the navigation frame and it is where the *navigation* takes place, for instance, inside of a building. The coordinate system used is known as the North-East-Up (NEU) and it coincides with the Cartesian system, denoted in this work as X-Y-Z.

Another important reference frame is the body frame. The body frame tells how the sensors are aligned with respect to the person. In this work, it is assumed that the body frame matches the natural axes of the body of the person, being the sensor coordinate x-y-z matched to the person's Forward-Right-Up axes respectively.

If the body frame is not aligned to the navigation frame, as shown in figure 2.3, an incorrect heading might be calculated leading to a false determination of the position of the person. To fix this problem, the inclination or tilt of the sensors should be determined and compensated *prior* to calculating the heading. Tilt

calibration is fully discussed in the next section.

2.2.3 Tilt Calibration

Caruso [8] proposed a tilt calibration method that has also been used by Fang [4] and Chen [6] as well. This method consists of finding the angles of deviation between the navigation and body frames, known as roll (β) and pitch (α), and illustrated in figure 2.3.
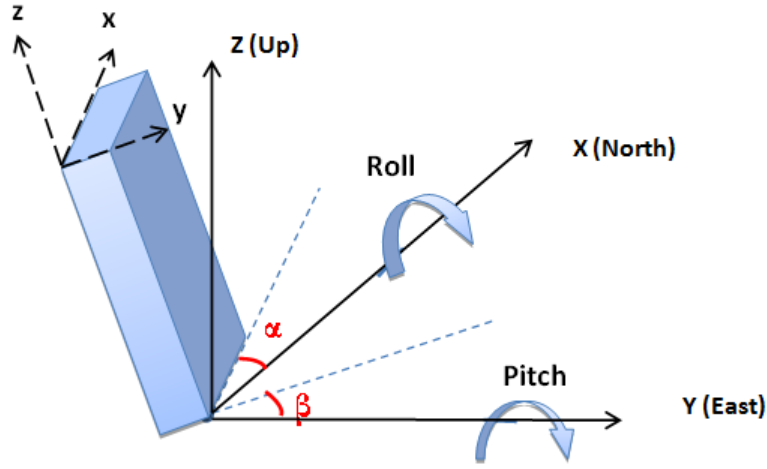

Figure 2.3: Definition of roll and pitch.

The β-angle can be found by rotating the object of interest around the X-axis and it is defined as the angle between the y-axis and the Y-axis. The α-angle can be found by rotating the object of interest around the Y-axis and it is defined as the angle between the x-axis and the X-axis.

If the phone is still or at rest, the information from the 3-axis accelerometer can be used to determine the roll and pitch angles. If the body frame is aligned with the navigation frame, the only acceleration measured by the accelerometers is the one corresponding to the gravitational force, noted for simplicity as g. The value of g would only be measured by the z-axis accelerometer, making the norm of the acceleration vector to be

$$||\mathbf{a}|| = \sqrt{a_{\mathrm{x}}^2 + a_{\mathrm{y}}^2 + a_{\mathrm{z}}^2} = g, \tag{2.4}$$

where $||\mathbf{a}||$ stands for the norm of the acceleration vector, and a_x, a_y, a_z stand for the acceleration values in their corresponding axis.
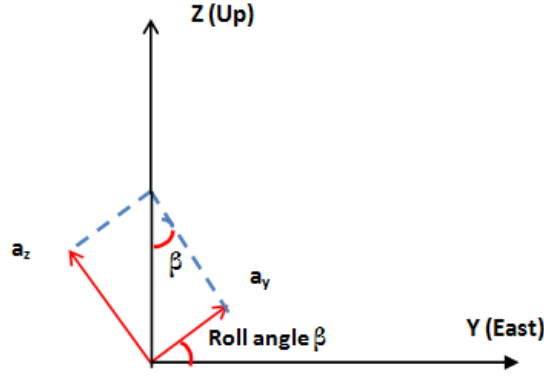

Figure 2.4: Calculation for roll angle β.

If the body frame is *not* aligned with the navigation frame, some information from g will be reflected in the other axes rather than only the z-axis. Using basic trigonometry, the roll and pitch angles can be found to be (refer to figure 2.4)

$$\beta = \arcsin\left(\frac{a_y}{||\mathbf{a}||}\right) \tag{2.5}$$

$$\alpha = \arcsin\left(\frac{a_x}{||\mathbf{a}||}\right). \tag{2.6}$$

Once the roll and pitch angles are known, the tilt can be compensated by rotating in roll and pitch using the matrices

$$\mathbf{M}_r = \begin{bmatrix} 1 & 0 & 0 \\ 0 & \cos\beta & \sin\beta \\ 0 & -\sin\beta & \cos\beta \end{bmatrix} \tag{2.7}$$

$$\mathbf{M}_p = \begin{bmatrix} \cos\alpha & 0 & -\sin\alpha \\ 0 & 1 & 0 \\ \sin\alpha & 0 & \cos\alpha \end{bmatrix}, \tag{2.8}$$

where $\mathbf{M}_r$ stands for the roll matrix, and $\mathbf{M}_p$ stands for the pitch matrix. The final rotation matrix ($\mathbf{M}_R$) can be obtained by multiplying

$$\mathbf{M}_R = \mathbf{M}_p \cdot \mathbf{M}_r. \tag{2.9}$$

In this particular case, the order of the matrix product do not alter the final result. The tilt-calibrated magnetic readings can be obtain multiplying

$$\mathbf{m}_R = \mathbf{M}_R \cdot \mathbf{m}, \tag{2.10}$$

where $\mathbf{m}$ is a vector containing the raw magnetic readings from the 3-axis magnetometer and $\mathbf{m}_R$ is a vector containing the tilt-calibrated measurements.
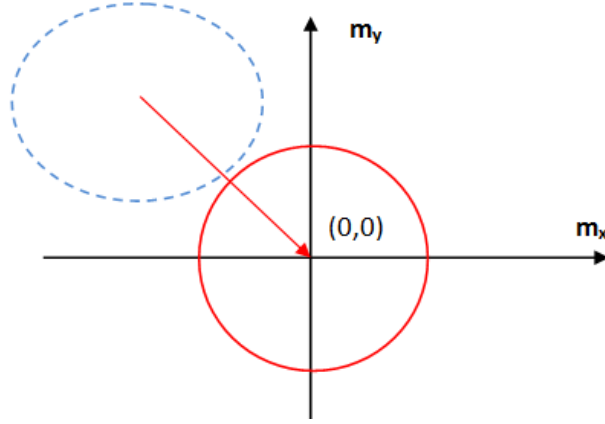
2.2.4 Static Calibration

Static disturbances can be generated by objects near to the magnetic sensors. In the case of pedestrians, disturbances could be generated by metallic objects or even the person itself. Ideally, if an xy-axis magnetometer is rotated 360° free of disturbance, its plot will look like the red circle centered in the origin in figure 2.5. In the presence of static disturbances, the result will show as an ellipsoid with an offset like the blue dotted ellipsoid in figure 2.5.

Caruso [8] proposes a method to compensate for static disturbances by first determining the scaling factors of the ellipsoid and then removing the offset. To fix the scaling factor, find the maximum and minimum magnetic values of the x and y magnetic readings and denote them as $x_{\max}$, $x_{\min}$, $y_{\max}$, and $y_{\min}$. Then find

$$X_{sf} = \max\left\{1, \frac{y_{\max} - y_{\min}}{x_{\max} - x_{\min}}\right\} \tag{2.11}$$

$$Y_{sf} = \max\left\{1, \frac{x_{\max} - x_{\min}}{x_{\max} - x_{\min}}\right\}, \tag{2.12}$$

where X_{sf} and Y_{sf} are scale factors and

Figure 2.5: Static Calibration.

$$X_{\text{off}} = \left[\frac{x_{\max} - x_{\min}}{2} - x_{\max} \right] X_{\text{sf}} \tag{2.13}$$

$$Y_{\text{off}} = \left[\frac{y_{\max} - y_{\min}}{2} - y_{\max} \right] Y_{\text{sf}}, \tag{2.14}$$

where X_{off} and Y_{off} are the offsets. Using the scale factor and the offset values, the static-calibrated magnetic readings can be found as

$$X_{\text{cal}} = X_{\text{sf}} \cdot m_{\text{x}} + X_{\text{off}} \tag{2.15}$$

$$Y_{\text{cal}} = Y_{\text{sf}} \cdot m_{\text{y}} + Y_{\text{off}}. \tag{2.16}$$

2.3   Disturbance Detector

As stated before, the proposed solution combines the gyroscope and the compass to find an accurate heading. In this section, a simple method that combines the gyroscope and compass information is used to detect dynamic disturbances.

Käppi [2] and Kim [9] proposed to compare the angular rates from the gyroscope and compass readings and to trust the gyroscope if there is any discrepancy. Since the gyroscope information is already in terms of angular rates, it is necessary to

derivate the heading from the compass to find its angular rate. This can be done as follows

$$\omega_{\text{compass}} = \frac{\psi_{\text{compass}}(t_k + \Delta t) - \psi_{\text{compass}}(t_k)}{\Delta t}, \tag{2.17}$$

where ω is the angular rate, ψ is the heading, and Δt is the time interval.

Another method proposed by Laddeto [7] is to discard fast variations in the magnetic readings until they stabilize again, since the compass information normally variates slowly.

2.4 The Kalman Filters

The Kalman filter is a mathematical tool developed by Rudolph E. Kalman in 1960 to make an estimation of an observed variable using a predictor-update set of equations [10]. If the noise is characterized as Gaussian and the problem where the filter is used can be represented as linear, the Kalman filter estimation is considered to be the optimal solution or the minimum squared error (MSE). In the nonlinear case, the Kalman filter has to be linearized and the solution is considered an *ad hoc* state estimator [10]. In the next sections, the linear and extended Kalman filters are described as well as some applications to the tracking problem by different authors.

2.4.1 The Linear Kalman Filter

In the linear case the motion and measurement models can be described by

$$\mathbf{x}_k = \mathbf{F}_{k-1}\mathbf{x}_{k-1} + \mathbf{G}_k\mathbf{u}_k + \mathbf{v}_{k-1} \tag{2.18}$$

$$\mathbf{z}_k = \mathbf{H}_k\mathbf{x}_k + \mathbf{w}_k, \tag{2.19}$$

where

$\mathbf{x}_k$ is the state vector,

$\mathbf{F}_{k-1}$ is the motion model matrix,

$\mathbf{G}_k$ is the control matrix,

$\mathbf{u}_k$ is the control input,

$\mathbf{v}_{k-1}$ is the motion noise,

$\mathbf{z}_k$ is the measurement vector,

$\mathbf{H}_k$ is the measurement matrix, and

$\mathbf{w}_k$ is the measurement noise.

The noises are independent from each other and their distribution can be described as

$$\mathbf{v}_{k-1} \sim N(\mathbf{0}, \mathbf{Q}_{k-1}) \tag{2.20}$$

$$\mathbf{w}_k \sim N(\mathbf{0}, \mathbf{R}_k), \tag{2.21}$$

where $\mathbf{Q}_{k-1}$ and $\mathbf{R}_k$ are known as the process and measurement noise covariance matrices respectively. The filtering algorithm can be divided in two sections, the prediction and the update. The prediction equations are

$$\hat{\mathbf{x}}_{k|k-1} = \mathbf{F}_{k-1}\hat{\mathbf{x}}_{k-1|k-1} + \mathbf{G}_k\mathbf{u}_{k|k-1} \tag{2.22}$$

$$\mathbf{P}_{k|k-1} = \mathbf{F}_{k-1}\mathbf{P}_{k-1|k-1}\mathbf{F}_{k-1}^{\mathrm{T}} + \mathbf{Q}_{k-1}, \tag{2.23}$$

where $\hat{\mathbf{x}}$ is the approximate mean and $\mathbf{P}$ is the measured covariance matrix of the variable of interest. The update equations are

$$\mathbf{K}_k = \mathbf{P}_{k|k-1}\mathbf{H}_k^{\mathrm{T}}(\mathbf{H}_k\mathbf{P}_{k|k-1}\mathbf{H}_k^{\mathrm{T}} + \mathbf{R}_k)^{-1} \tag{2.24}$$

$$\hat{\mathbf{x}}_{k|k} = \hat{\mathbf{x}}_{k|k-1} + \mathbf{K}_k(\mathbf{z}_k - \mathbf{H}_k\hat{\mathbf{x}}_{k|k-1}) \tag{2.25}$$

$$\mathbf{P}_{k|k} = (\mathbf{I} - \mathbf{K}_k \mathbf{H}_k)\mathbf{P}_{k|k-1}, \tag{2.26}$$

where $\mathbf{K}$ is the gain used to weight the measurement against the prediction. The prediction equations find the *a priori* distribution by *predicting* the mean and variance of the next value of the observed variable. In the case of the update equations, they calculate the *posterior* distribution by using the new weighted measurements.

2.4.2 The Extended Kalman Filter

In the nonlinear case the motion and measurement models can be described by

$$\mathbf{x}_k = \mathbf{f}(\mathbf{x}_{k-1}, \mathbf{u}_k) + \mathbf{v}_{k-1} \tag{2.27}$$

$$\mathbf{z}_k = \mathbf{h}(\mathbf{x}_k) + \mathbf{w}_k, \tag{2.28}$$

where $\mathbf{f}(\mathbf{x}_{k-1})$ and $\mathbf{h}(\mathbf{x}_k)$ are the nonlinear functions that describe the motion and the measurement models respectively. The filter equations are given by

$$\hat{\mathbf{x}}_{k|k-1} = \mathbf{f}(\hat{\mathbf{x}}_{k-1|k-1}, \mathbf{u}_{k|k-1}) \tag{2.29}$$

$$\mathbf{P}_{k|k-1} = \mathbf{F}_{k-1}\mathbf{P}_{k-1|k-1}\mathbf{F}_{k-1}^{\mathrm{T}} + \mathbf{Q}_{k-1}, \tag{2.30}$$

$$\mathbf{K}_k = \mathbf{P}_{k|k-1}\mathbf{H}_k^{\mathrm{T}}(\mathbf{H}_k\mathbf{P}_{k|k-1}\mathbf{H}_k^{\mathrm{T}} + \mathbf{R}_k)^{-1} \tag{2.31}$$

$$\hat{\mathbf{x}}_{k|k} = \hat{\mathbf{x}}_{k|k-1} + \mathbf{K}_k(\mathbf{z}_k - \mathbf{h}(\hat{\mathbf{x}}_{k|k-1})) \tag{2.32}$$

$$\mathbf{P}_{k|k} = (\mathbf{I} - \mathbf{K}_k \mathbf{H}_k)\mathbf{P}_{k|k-1}. \tag{2.33}$$

The equations are practically the same as the linear case, except that in the case of the state prediction and update, it is the nonlinear function what is used instead of the matrix multiplication. In the case of the projected error covariance and update covariance, it is necessary first to linearize the nonlinear expressions. This can be achieved by finding the Jacobian matrices of the partial derivatives of f and h with respect to x as follows:

$$\mathbf{F}_{[i,j]} = \frac{\delta f_{[i]}}{\delta x_{[j]}}(\hat{x}_{k-1|k-1}, u_k) \tag{2.34}$$

$$\mathbf{H}_{[i,j]} = \frac{\delta h_{[i]}}{\delta x_{[j]}}(\hat{x}_{k|k-1}). \tag{2.35}$$

Note that the subindex k has been dropped from the matrix notation to make it easier to read.

2.4.3 Kalman Filter Models

The tracking problem is certainly not new and several authors have already proposed models to solve it. Chen [6] proposed to combine accelerometers and magnetometers in an extended Kalman filter, and Jirawimut [12] proposed another one that uses a GPS to aid in the step size and compass bias error correction. Both setups have proven to work on outdoor conditions, but they do not deal with magnetic disturbances indoors.

On a different application, Foxlin [11] proposed to use accelerometers, magnetometers, and gyroscopes to track the movement of the head of a person. His approach uses a complimentary Kalman filter to correct the heading and compensate for the gyroscope errors. This application could be modified to suit the needs of this project, but Foxlin assumes that the gyroscope errors are known and that they are used as a constant in the filter algorithm.

Laddeto [7] and Kim [9] proposed to implement a Kalman filter that combines the gyroscopic and magnetic information considering their strengths and weaknesses, and also environments where magnetic disturbances could be present. Based on this idea, a simple Kalman filter with disturbance detector was designed for this master thesis. The implementation of the entire system is described in chapter 3.

Chapter 3

Implementation

S OLUTIONS by other researchers were briefly introduced and discussed in the previous chapter. In this chapter, a solution is proposed using a single algorithm for distance and heading estimation. Also, the disturbance detector and kalman filter are discussed in detail.

3.1 Distance Estimation

The step detection and step length estimation were discussed in 2.1. Chen [6] compared the linear and nonlinear step estimation performances. His conclusions were that the error from the step length estimation does not influence the positioning accuracy severely. Therefore, the nonlinear model was chosen for this work. In section 3.1.1 the step detection implementation is discussed, and in section 3.1.2 the step length estimation is presented.

3.1.1 Step Detection

Fang [4] mentions that natural walking speed has a frequency of less than 3 Hz. Figure 3.1 shows the frequency spectrum for the z-axis raw acceleration data of one experiment in this project. It can be seen that the main frequency is around 1.8 Hz and that there are harmonics every 0.9 Hz. To reduce random variations

and get rid of most of the secondary peaks, a low pass filter can be used. Following Fang's idea, an 8-sample moving average was implemented

$$\bar{a}_z(t) = \frac{1}{8} \sum_{i=t-7}^{t} a_z(i),\tag{3.1}$$

where $a_z(i)$ is the raw acceleration sample and $\bar{a}_z(t)$ is the filtered or averaged result. The result of the filter is also shown in figure 3.1. It can be seen that the component in 1.8 Hz remains while the others are attenuated or even eliminated.
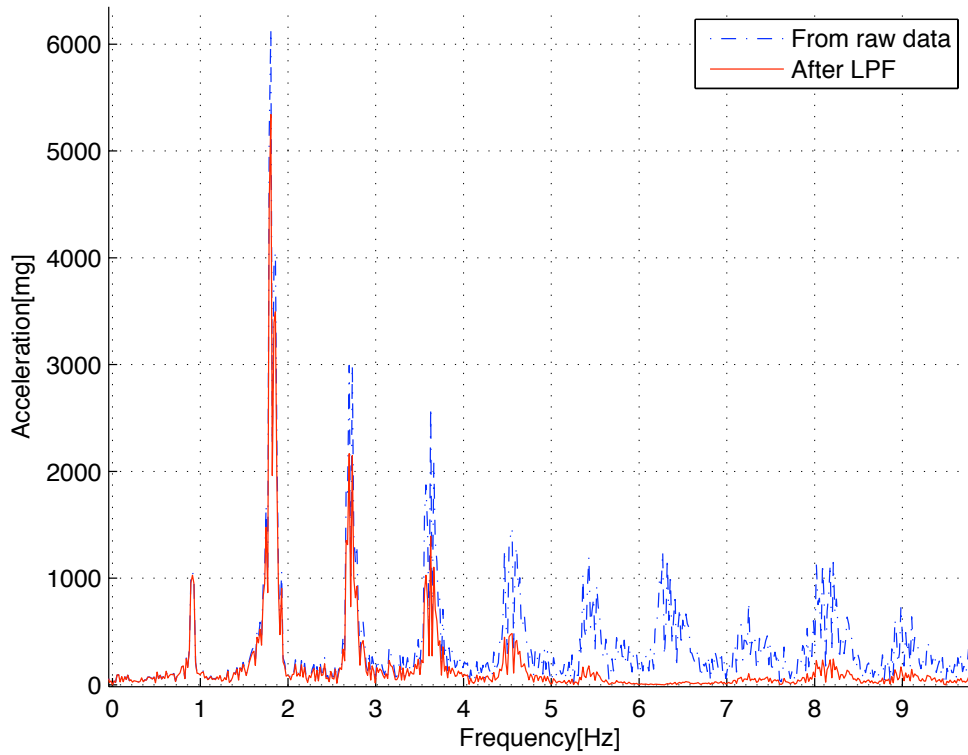

Figure 3.1: Frequency spectrum of the z-axis acceleration signal before and after filtering.

After filtering the acceleration samples, the offset of the signal is removed and the negative to positive transitions are marked as the start of each step. Then, the maximum and minimum values within each step are marked as shown in figure 3.2.

Marking all the negative to positive transitions is not enough to determine the number of steps given by the person. Sometimes the signal can have fast zero-crossings that do not represent a step. These crossings could be caused by different factors such as the gait of the person. A threshold was defined to distinguish between real and false step detections. Figure 3.2 also shows a fast negative to positive transition within the first detected step. This was discarded with the aid of the threshold.

Figure 3.2: Step detection and max/min values are marked. The figure also shows a fast zero-crossing transition that was discarded by thresholding.

3.1.2   Step Length Estimation

Once the steps are defined and their maximum and minimum acceleration values are known, equation (2.1) can be used to find the length of each step. The equation is repeated here for convenience

$$L_{\text{step}} = k \cdot \sqrt[4]{A_{\text{max}} - A_{\text{min}}}.$$

The k value can be adjusted per person or it can also be fixed depending on the accuracy that is required. In this work, to calibrate k the user walked a known distance and then the least squares method was used to find the value that would give the best distance estimation.

3.2   Heading

The way the heading is obtained from the gyroscope and magnetometers was entirely described in section 2.2. This section is divided in two short parts: the first one deals with the heading calculation using the magnetometers, and the second one with the adjustment that is needed for the Kalman filter to operate.

3.2.1   Heading Calculation

After the tilt and static calibrations are performed, the heading is found using equation (2.3). Figure 3.3 shows the result. It can be seen that the compass assigns headings only from 0 to 2π radians. When the heading 'jumps' from 2π to 0 radians or viceversa, the signal exhibits a discontinuity that looks like an extremely fast transition. For instance, refer to the sample range between 6000 and 8000 in the figure.
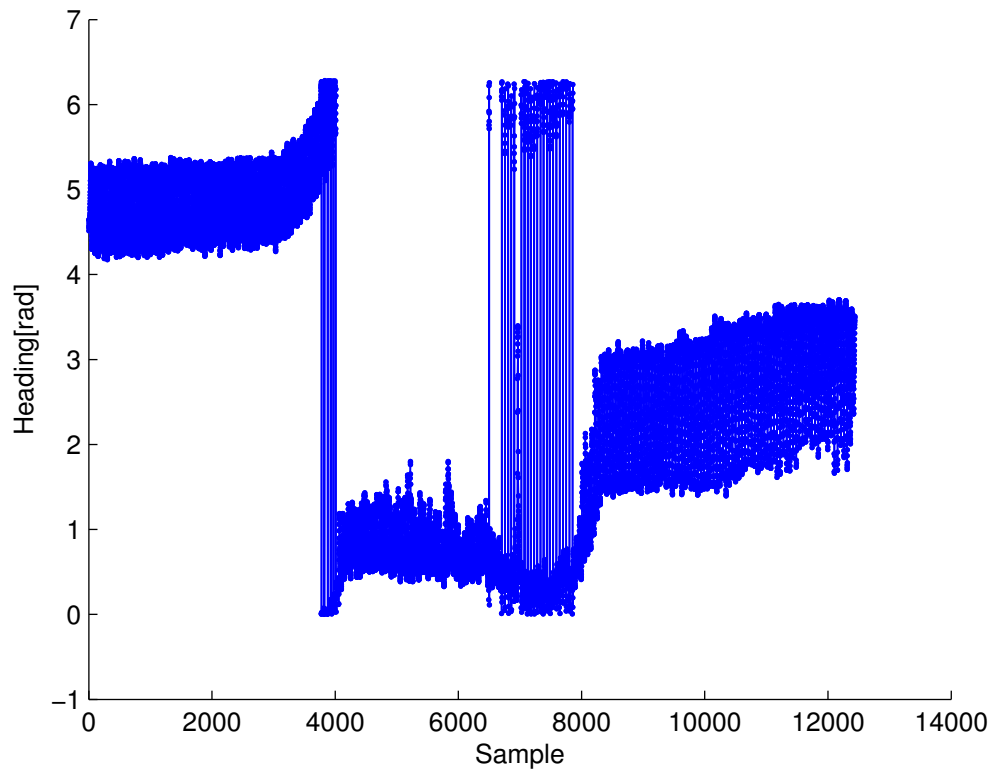
Figure 3.3: Raw heading from the compass.

3.2.2 Heading Adjustment

In this section, the resulting compass signal is adjusted so that it can be processed by the Kalman filter. Since the Kalman filter rely on previous information to predict the next value, it is key to create a *continuous* signal with the same information as the compass signal.

Knowing that the compass samples *do not* represent the heading per step, it can be found as the average of all the compass samples within one step. This averaging can bring new issues, for instance: if a person is walking north, the compass samples will be around 0 radians with a certain variation. This variation is denoted by the red-dashed lines on figure 3.4. It can be seen that the values will 'jump' between 0 and 2π. Averaging these values will give a result around π, which represents
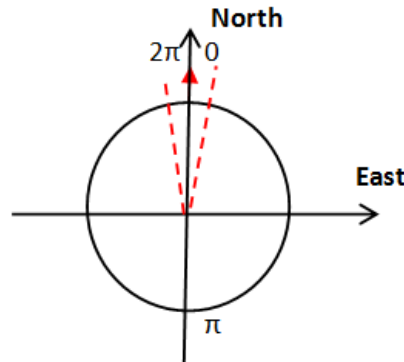
Figure 3.4: Heading range variation when the person is heading north.

south. To solve this problem, a 3-step adjustment is proposed:

1. **Adjust the heading in each step.**
   First, calculate the variance of the heading in each step. If the variance is larger than a given threshold, it means that the step is towards the north direction and that the heading is 'jumping' between 0 and 2π. After the 'jump' is detected in the step, add 2π to all the values in the first quadrant that are *close* to zero (the level of *closeness* is defined experimentally). The top plot of figure 3.5 shows an example of areas with discontinuities. The bottom plot of figure 3.5 shows the result of the adjustment.

2. **Adjust the heading *between* steps.**
   After the first adjustment has been done, the signal has continuity within each step. Now, the entire signal has to be checked to make sure that there are no discontinuities *between* the steps. The top plot of figure 3.6 shows an example of discontinuities between the steps.

   The first thing to do is to calculate the heading per step. The result is shown in the top plot of figure 3.7. Then, two checks are made: (a) if the heading variance between neighboring steps is larger than a certain threshold, and (b) if the variance of the sine of the heading between neighboring steps is smaller than another threshold.

   If (a) is met, it means that there is a 'jump' to consider. If (b) is met, then that 'jump' is a discontinuity and 2π must be added or subtracted to the rest of the signal in order to keep continuity. Once the discontinuities are
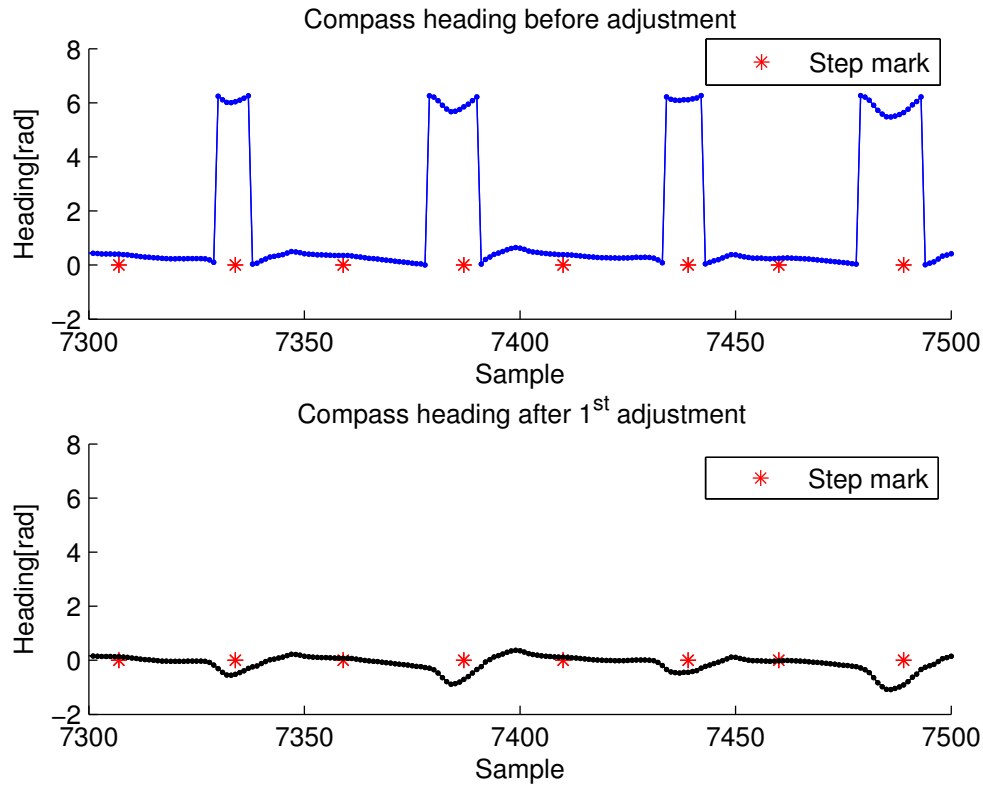
Figure 3.5: Heading comparison before (top) and after (bottom) the first adjustment.

removed, the heading per sample will look like the bottom plot of 3.6. The bottom plot of figure 3.7 shows how the heading per step would look.

3. **Make the compass signal follow the trend of the integrated gyroscope signal.**
   In the case that the person turns for more than 360°, the signal must be adjusted so that 0 and 2π are no longer the boundaries of the signal. The gyroscope integrated signal is a good example for the new compass signal to follow. This is achieved by adding or subtracting 2π as shown in figure 3.8.

Figure 3.6: Compass heading per sample after the first (top) and second (bottom) adjustments.
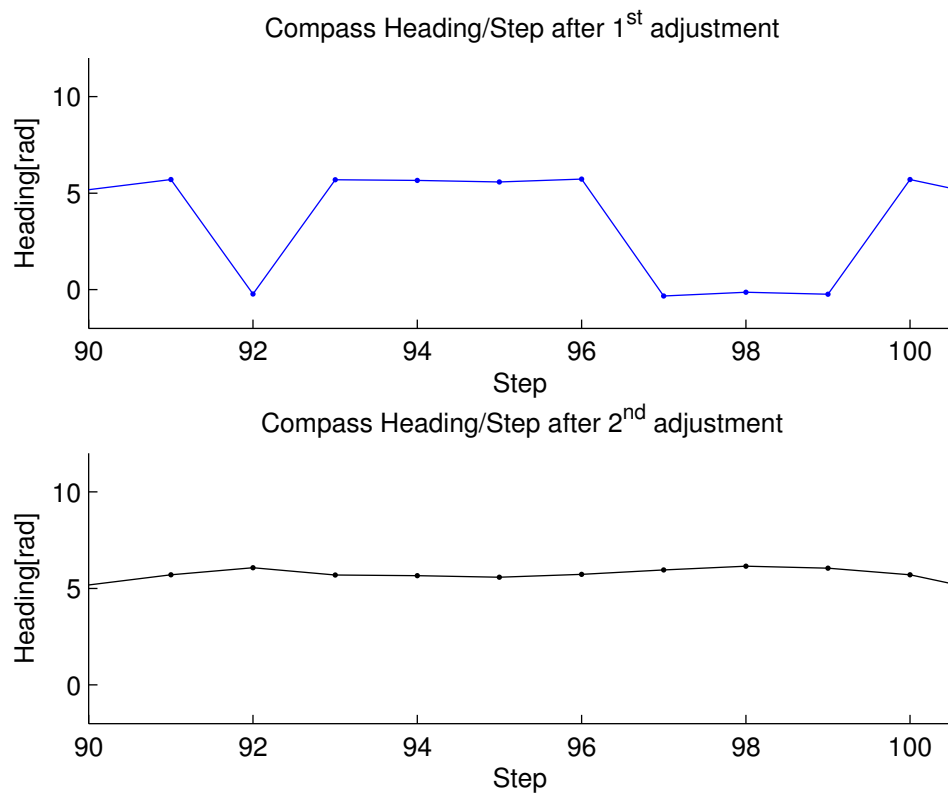
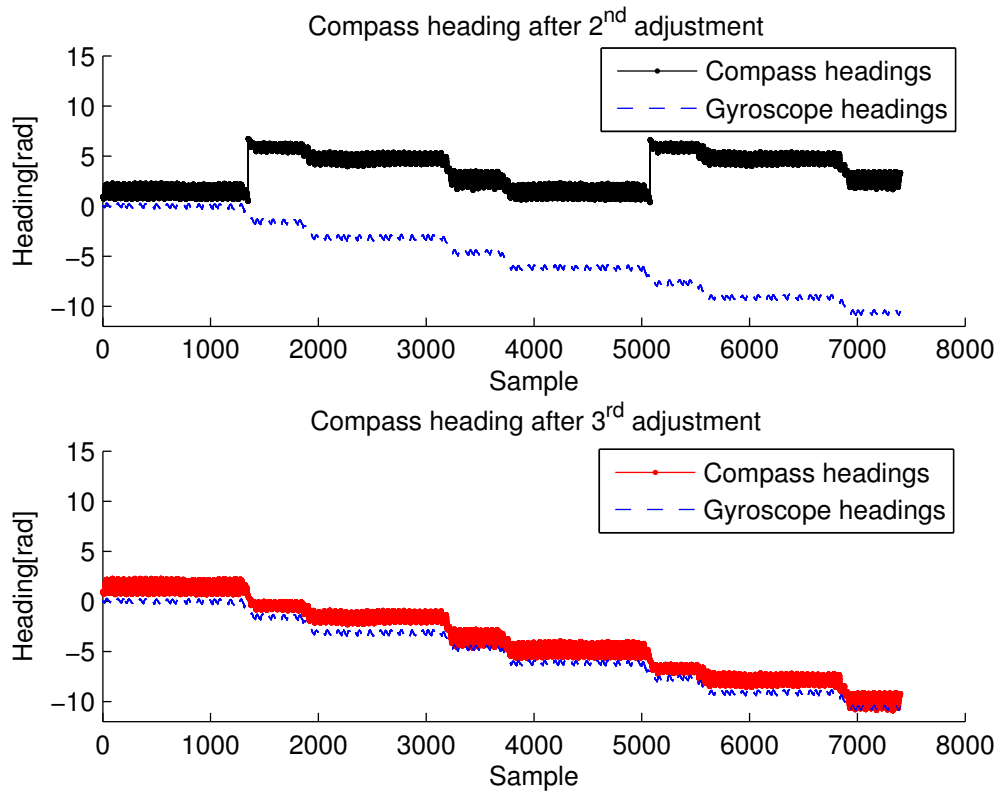**Figure 3.7:** Compass heading per step after the first (top) and second (bottom) adjustments.

Figure 3.8: Compass heading per sample after the second (top) and third (bottom) adjustments.

3.3   Disturbance Detector

In this master thesis, the angular rate detector mentioned in chapter 2 was implemented and compared to a 3-axis magnetic magnitude (m2) detector. The m2-detector was implemented by obtaining average magnitude measurements *per step*, and comparing them against thresholds. The thresholds were defined doing tests in disturbance-free areas. If the magnitudes were over the threshold values, the signal during that step was considered to be disturbed. Figure 3.9 shows an indoor experiment where the disturbances are categorized in low/none, medium, and high, using the thresholds mentioned before.
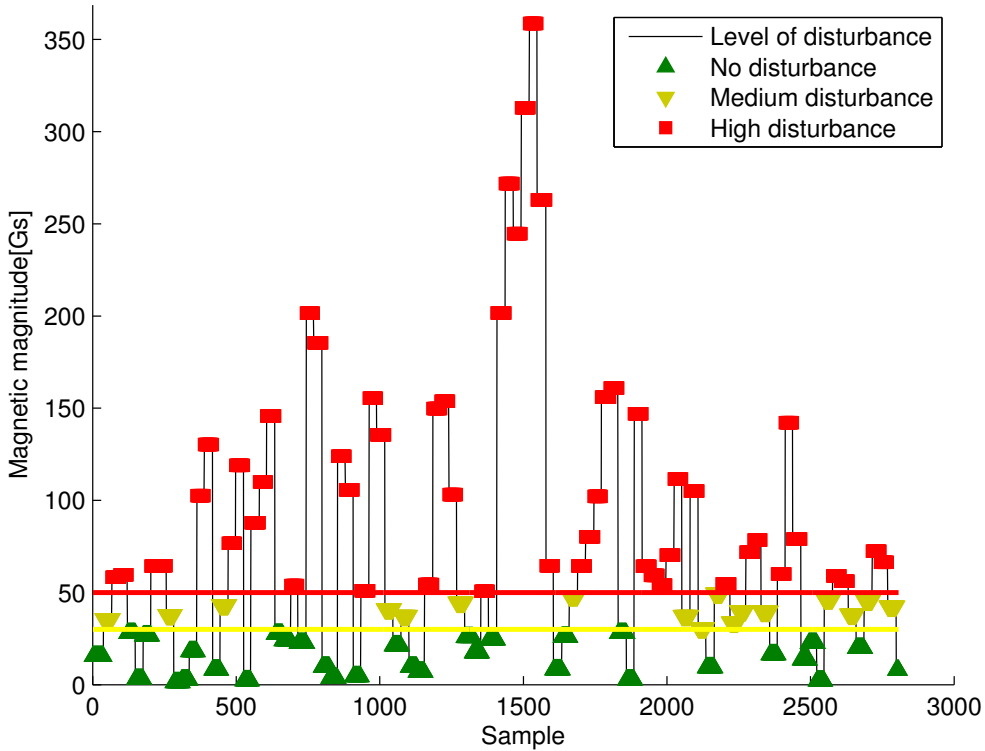

Figure 3.9: m2-detector.

The method mentioned by Käppi and Kim, where the angular rates from the gyroscope and compass are compared, is shown in figure 3.10. It can be seen that when there is no disturbance, the compass follows the gyroscope's angular rate. To detect whether there is a disturbance or not, it is necessary to find the difference of

both signals and define a threshold. Figure 3.11 shows an example of a disturbance found with the aid of the gyroscope and the threshold.
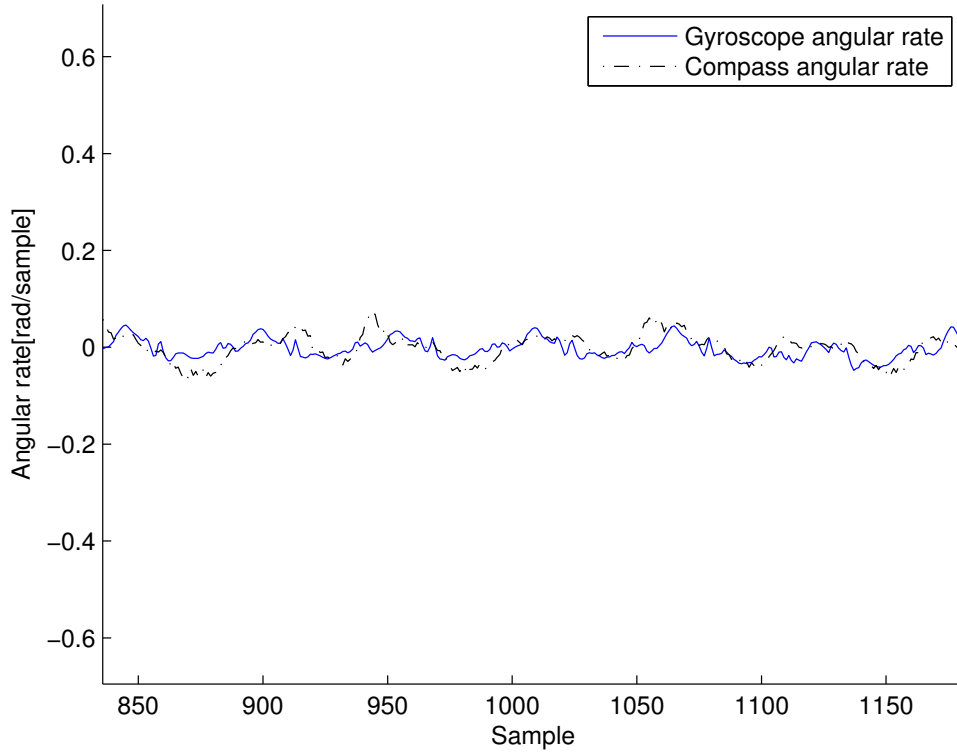

Figure 3.10: Comparison of compass and gyroscope's angular rates.

Both methods were compared to verify their performance. In figure 3.12, it can be seen that the detectors do not coincide in their results. Only the angular rate detector was used in the final solution because

3.4 Kalman Filter

Since the compass and the gyroscope cannot solve the positioning problem on their own, another solution must be designed. In this section, the authors introduce a simple sensor fusion algorithm based on the Kalman filter. Consider again the equations 2.18 and 2.19, repeated here for convenience
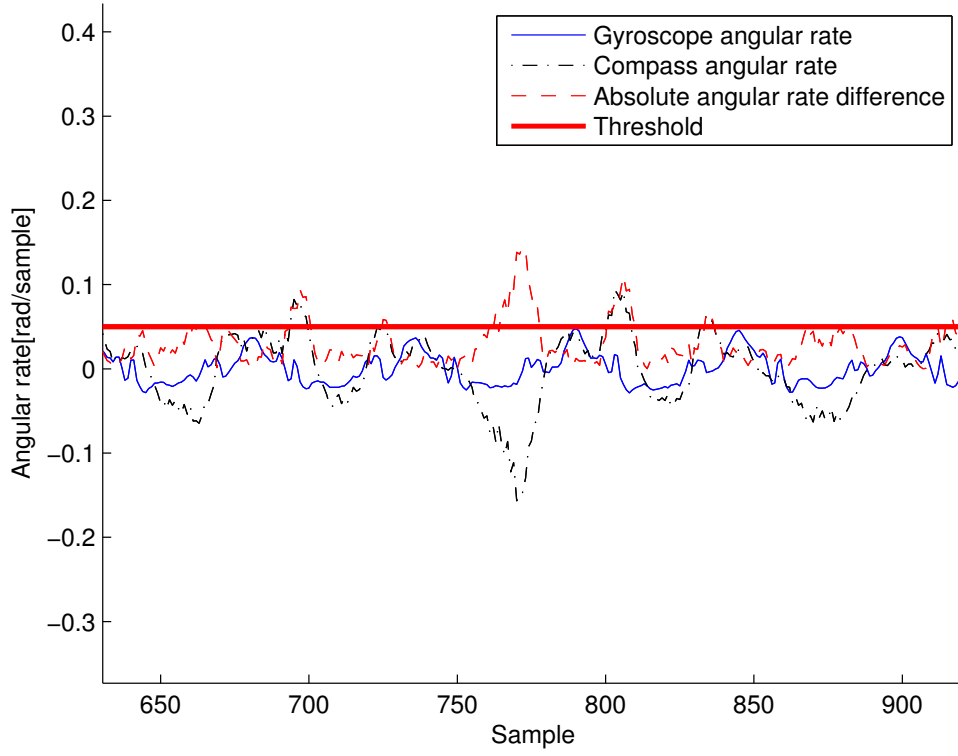
Figure 3.11: Angular rate detector.

$$\mathbf{x}_k = \mathbf{F}_{k-1}\mathbf{x}_{k-1} + \mathbf{G}_{k-1}\mathbf{u}_k + \mathbf{v}_{k-1}$$
$$\mathbf{z}_k = \mathbf{H}_k\mathbf{x}_k + \mathbf{w}_k.$$

In this work, the model is linear and consists of a single equation

$$\phi_k = \phi_{k-1} + \Delta t \cdot \omega_k + v_{k-1}^{\phi}, \tag{3.2}$$

note that ϕ_k is the state variable, ω_k is the control input, $\mathbf{F} = 1$, $\mathbf{G} = \Delta t$, and v_k^{ϕ} is the process noise. The measurement model is then given by

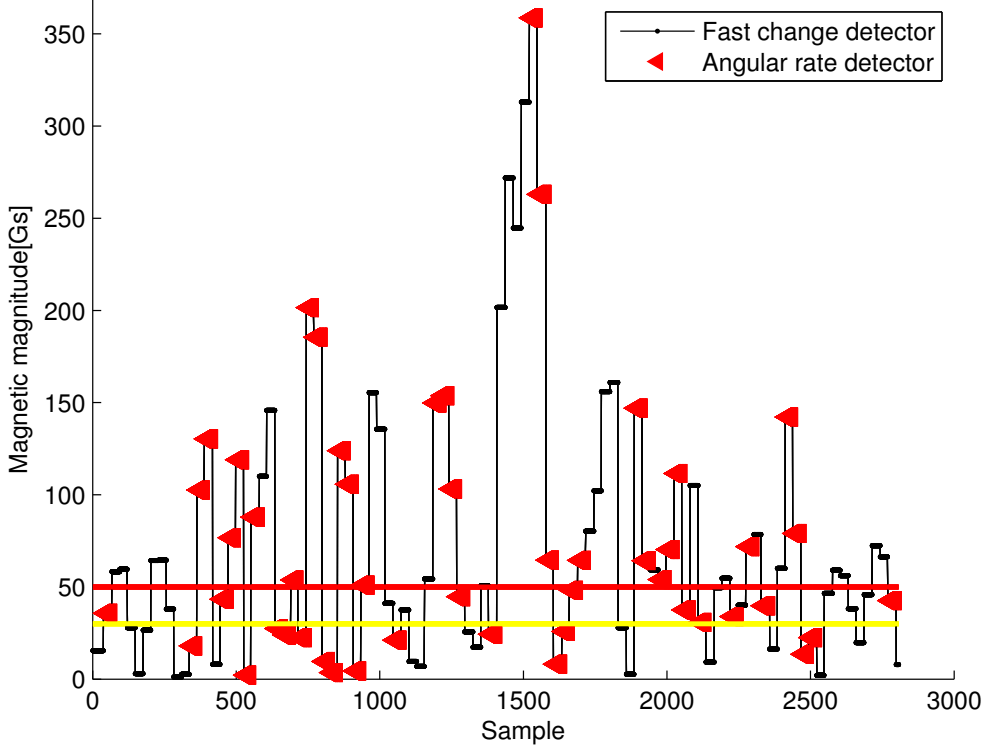$$z_k = \phi_k + v_k^z, \tag{3.3}$$

29

Figure 3.12: Comparison between both disturbance detectors.

where $\mathbf{H} = 1$ and v_k^z is the measurement noise.

The measurement is given by the heading of the compass ϕ_k, while the angular rate of the gyroscope is used as the control input ω_k. During the Kalman filter iterations, the angular rate from the gyroscope and the compass is compared to detect disturbances. When the disturbance flag is clear, this configuration sums the gyroscope's angular rate to the heading given by the compass. When the disturbance flag is set, the algorithm integrates the gyroscope to the last good compass sample.

The integration of the gyroscope, compass, and disturbance detector reduce the overall magnetic interference on the system. Also, the gyroscope bias drift effect is reduced by integrating the gyroscope to the compass heading and not the gyroscope alone.

Chapter 4

Experiments

T HIS CHAPTER deals with the the experiments that were carried out. First, the hardware and software used to acquire the sensor information and to implement the solution are metioned. Then, the experiment conditions are described and the experiment results are presented. The issues that were found are discussed in the end of the chapter.

4.1 Hardware and Software

To make the experiments, the authors used the STEVAL-MKI062V2 demostration kit by ST Microelectronics® -also known as the iNEMO™ board. The board consists of accelerometers, gyroscopes, magnetometers and pressure and temperature sensors. The complete board specifications can be found in [16].

The sensors that were used for this work are the 3-axis accelerometer, the 3-axis magnetometer, and the 1-axis yaw gyroscope. The board was mounted on a phone chassis to emulate a real phone and to be able to test the system under real conditions. Figure 4.1 shows the setup.

The sensor configuration and acquisition was done through the graphical user interface (GUI) provided with the iNEMO™ board. The GUI generates a text file with all the sensor information that can be later used for offline processing. MATLAB™ [17] was used to process the sensor information.
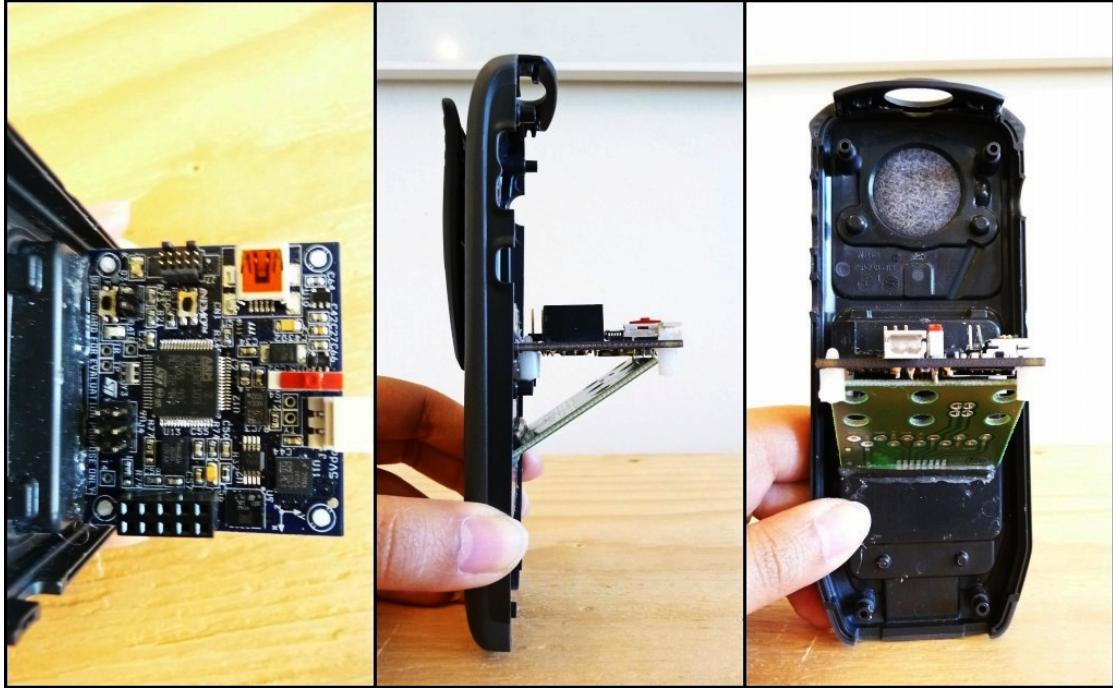
Figure 4.1: Hardware setup for the experiments.

4.2 Experiment Conditions

Three positions were considered for the experiments: on the waist, on the left side of the left pocket, and on the center of the left pocket. The positions can be seen on figure 4.2. Different positions were used to analyze the effect on the sensor data. The complete setup needs the user to carry a laptop computer connected to the iNEMO™ board to act as power supply and to store the sensor information. Figure 4.3 shows the setup. Different persons were used to test the algorithm, as well as different indoor and outdoor scenarios.

Figure 4.2: Phone positions: (left) on the waist, (center) on the left side of the left pocket, and (right) on the center of the left pocket.

Figure 4.3: Complete experiment setup.

4.3   Results

4.3.1   Outdoor

This section shows the result of a single outdoor experiment. The purpose of this experiment was to verify the reliability of the compass in areas where magnetic disturbances are at minimum levels. Figure 4.4 shows the trajectory (map courtesy of Google Maps® [18]) and table 4.1 shows the results. This test was performed by a man and the phone was positioned in the waist. It can be seen that the compass trend is close to the travelled path but the trajectory is considerably different from the original path. The combination of the gyroscope and compass into the Kalman filter gives a better result.
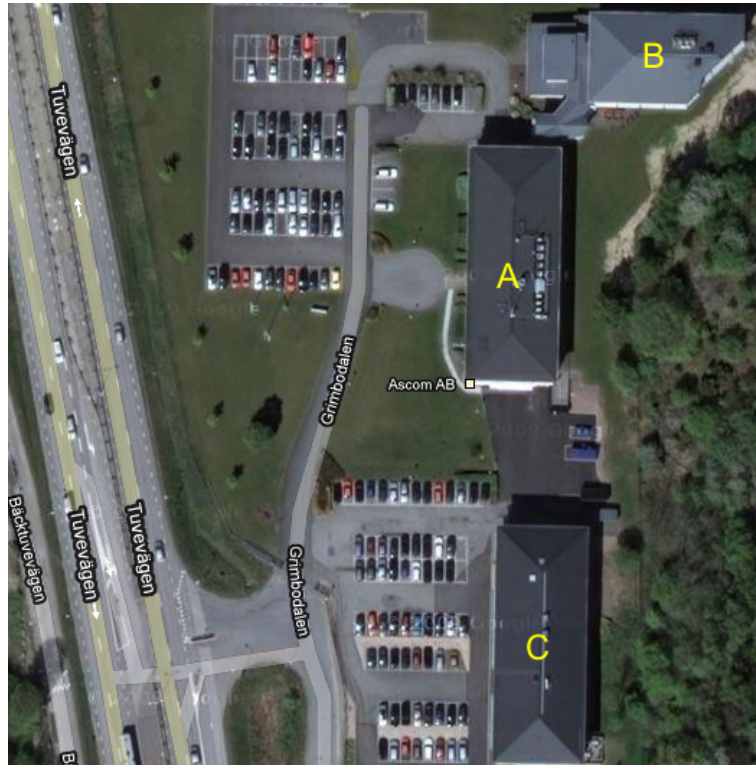

Figure 4.4: Outdoor experiment in Slottsskogen, Göteborg, Sweden.

Table 4.1: Outdoor experimental results.

Distance[1]	Estimated Distance	Distance Error Rate	Max Error Position	Max Error Rate in Position
370 m	348 m	6.3 %	11.8 m	3.2 %

4.3.2 Indoor

In this section, the results of the indoor experiments are shown. Experiments were carried out at ASCOM's offices in Göteborg, Sweden. A satellite picture of the facilities is shown in figure 4.5 (courtesy of Google Maps®). The building names are marked on each one of them.

Figure 4.5: ASCOM offices in Göteborg, Sweden.

For convenience, the experiments were named from 1 to 5 and ordered by distance:

1. Building B, second floor (figure 4.6).
   Man. Phone in the waist.

2. Building A, second floor (figure 4.7).
   Woman. Phone in the pocket.

3. Building C, third floor (figure 4.8).
   Woman. Phone in the pocket.

4. Building A and the connecting passage of building B, second floor (figure 4.9).
   Woman. Phone in the waist.

5. Buildings A and B, second floor (figure 4.10).
   Man. Phone in the waist.

Table 4.2 shows the results obtained for the Kalman filter implementation. For all the experiments, the $\mathbf{R}$ and $\mathbf{Q}$ matrices were found empirically and chosen to be the same. Also, the disturbance threshold was fixed even though buildings C and B proved to be under more severe disturbances in comparison to building A. For instance, look at how the compass-only solution of experiment 3 (figure 4.8) gets out of the map just after a few meters were walked.

Table 4.2: Indoor experimental results.

Exp.	Distance[1]	Estimated Distance	Distance Error Rate	Max Error Position	Max Error Rate in Position
1	91 m	86.2 m	5.5 %	1.4 m	1.5 %
2	92.3 m	90.7 m	1.8 %	4.3 m	4.6 %
3	105.6 m	102.2 m	3.3 %	3.4 m	3.2 %
4	166.4 m	167.1 m	0.04 %	5.2 m	3.1 %
5	193 m	204.8 m	6.1 %	13 m	6.7 %

---

[1]The distance was calculated based on a *perfectly* straight path. The *real* path walked by the person might differ by a few meters.
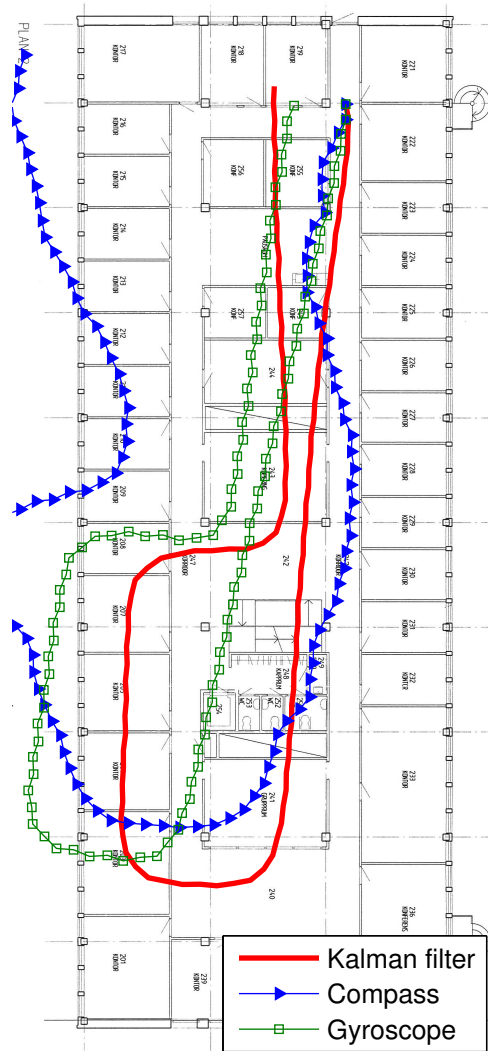
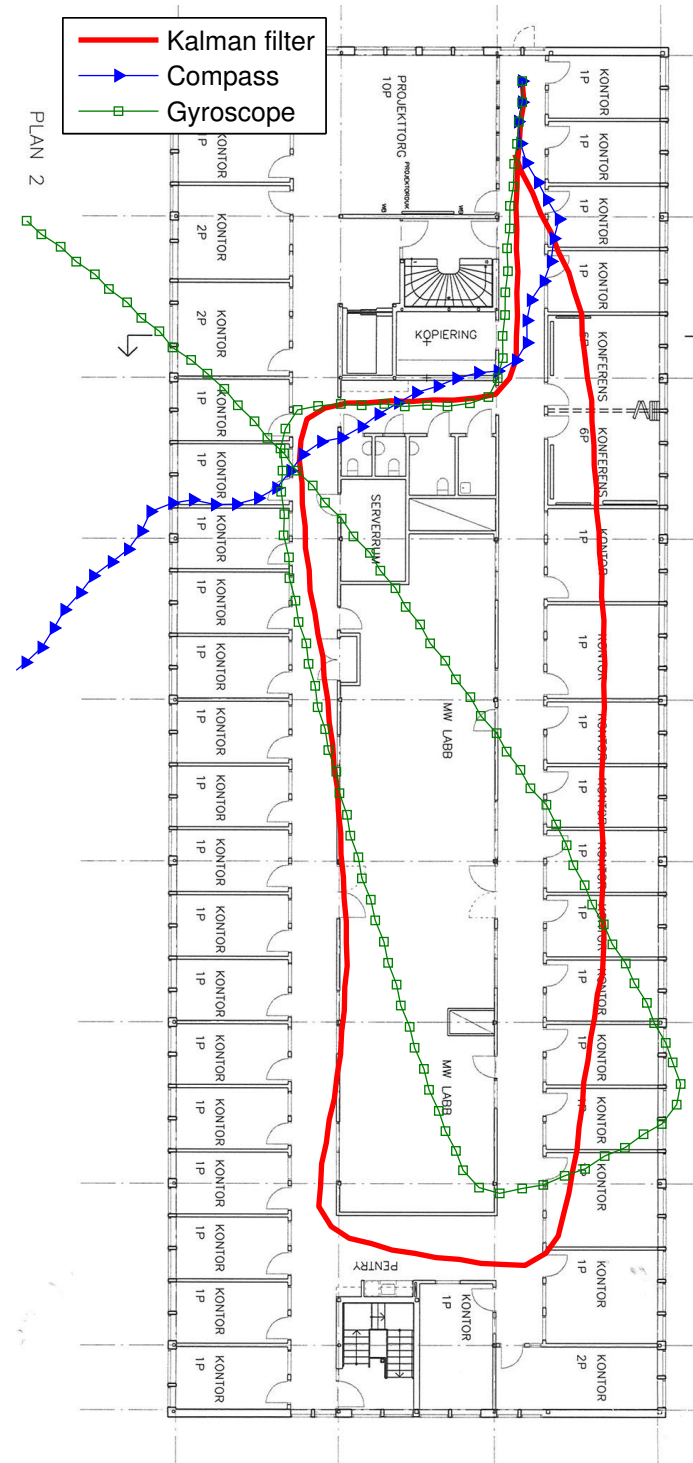**Figure 4.6:** Experiment 1.

Figure 4.7: Experiment 2.

Figure 4.8: Experiment 3.
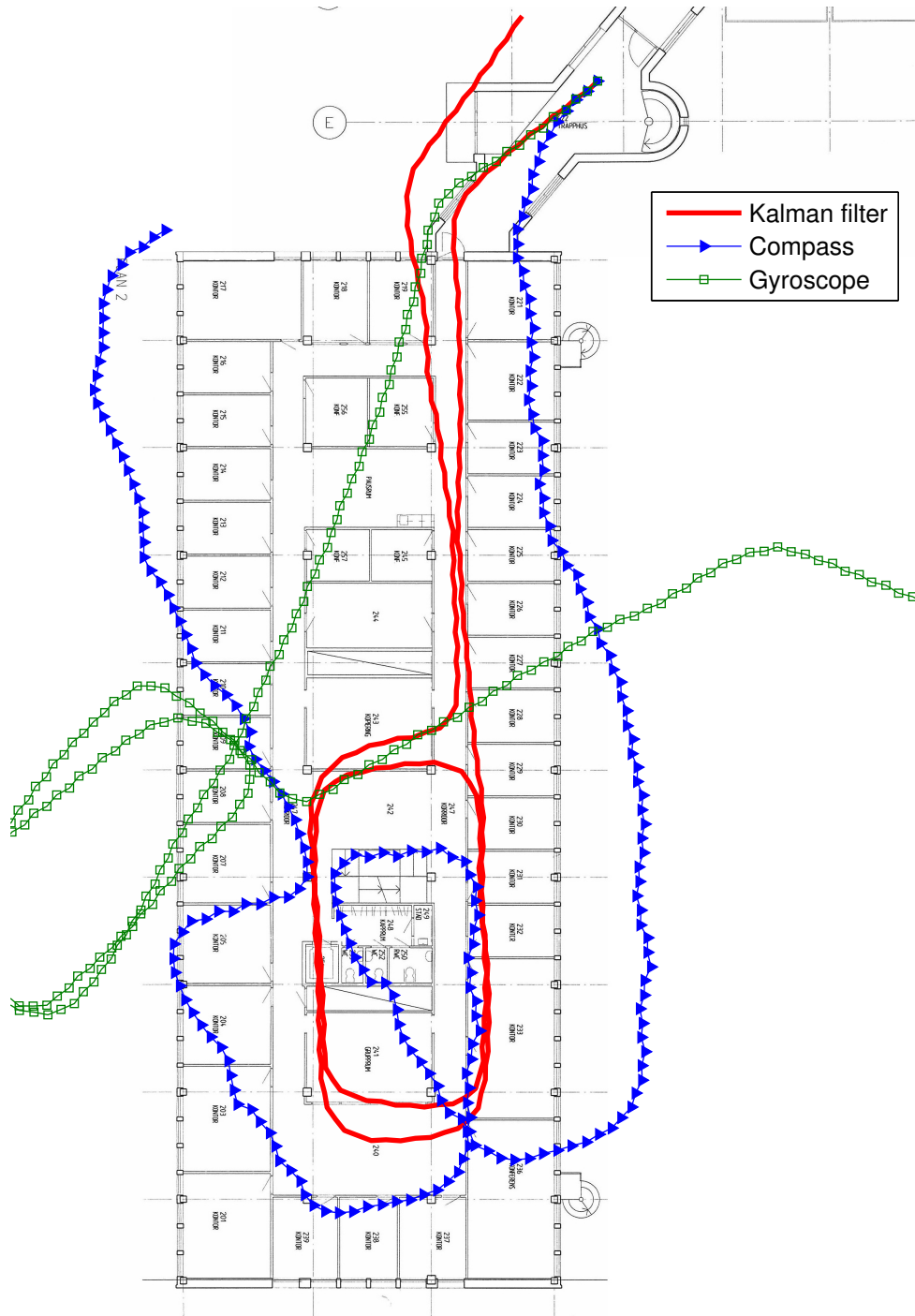
Figure 4.9: Experiment 4.

Figure 4.10: Experiment 5.

4.4 Issues

4.4.1 Phone Movement

If the phone position is moved during the experiment, the sensor information will be affected. The phone movements depend mainly on the person's walking gait and where the phone is located in the body.

The human gait is cyclical but is different from person to person. An example of how the gait changes the sensor information can be seen on figure 4.11. In this figure, the acceleration data of two different subjects is compared.
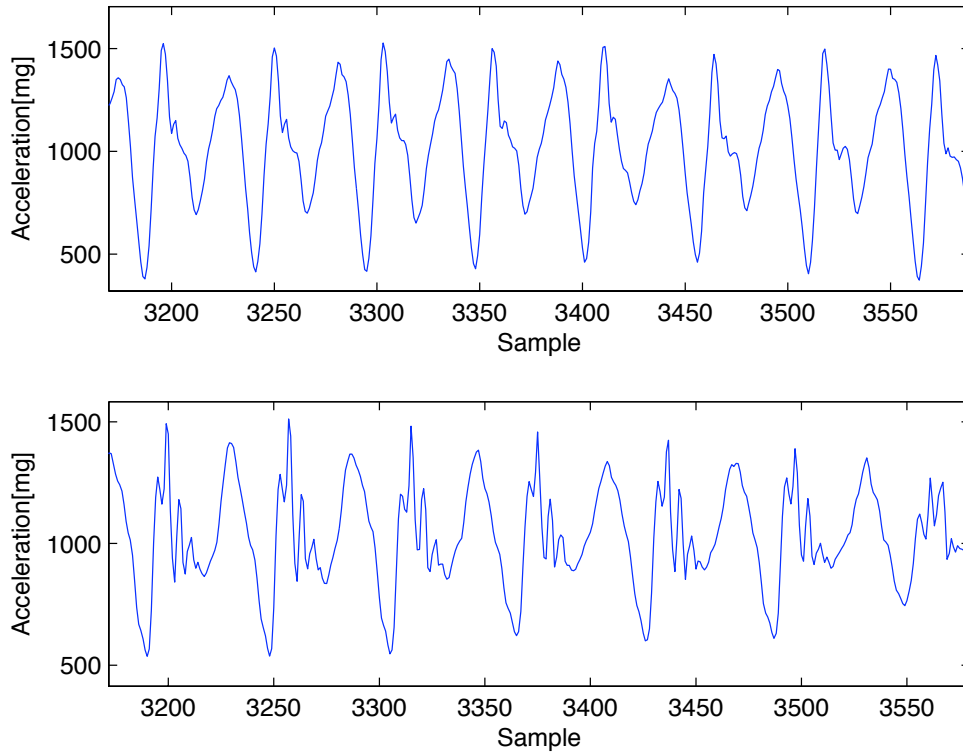

Figure 4.11: Accelerometer signal comparison between two subjects.

Different parts of the body are subject to different oscillations and force magnitudes while walking. If the phone is located on the waist, it will be subject to a different

force than if it is located on the hand or chest. Experiments 2 and 4 use the same subject but the phone is located on different places. It can be seen that the gyroscope gets most of the impact. However, the Kalman filter was able to recover the trajectories in these cases.

Phone rotations in the middle of the experiments would change the inclination of the phone. This would invalidate the tilt calibration and affect the magnetometer information. Also, since only a single gyroscope is used, the sensor could be fooled to believe that the user turned for a longer period of time or for a bigger angle. Figure 4.12 shows a case where the phone rotates and the sensor data becomes unreliable.

4.4.2 The Magnetic Disturbances

The magnetic disturbances and the disturbance detectors were introduced and discussed in sections 2.3 and 3.3. As it was said before, the disturbance detector is a good tool for *detecting* false direction changes on the compass and to ignore them. The problem arises when the signal is disturbed, but the disturbance detector is *not* triggered. It is possible for the system to be under small disturbances that change the heading information without triggering the detector. In such cases, the Kalman filter would still trust the compass, resulting in bad performance. Figure 4.13 shows an example were the gyroscopic information is relatively good but the Kalman filter is not because of undetected disturbances.
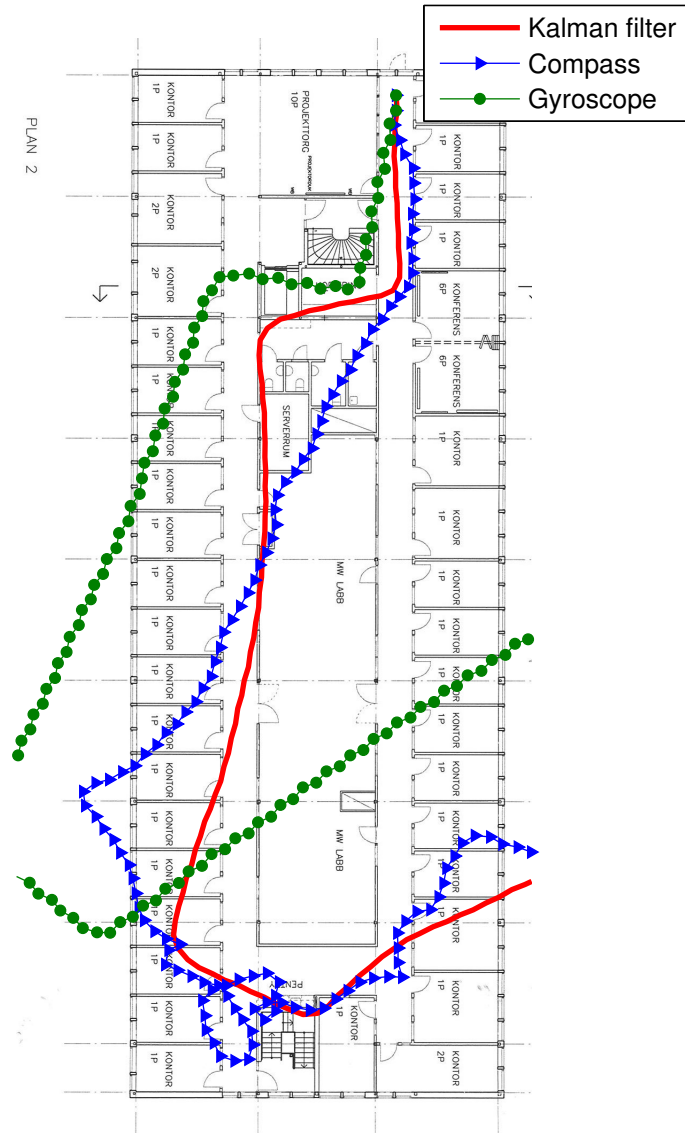
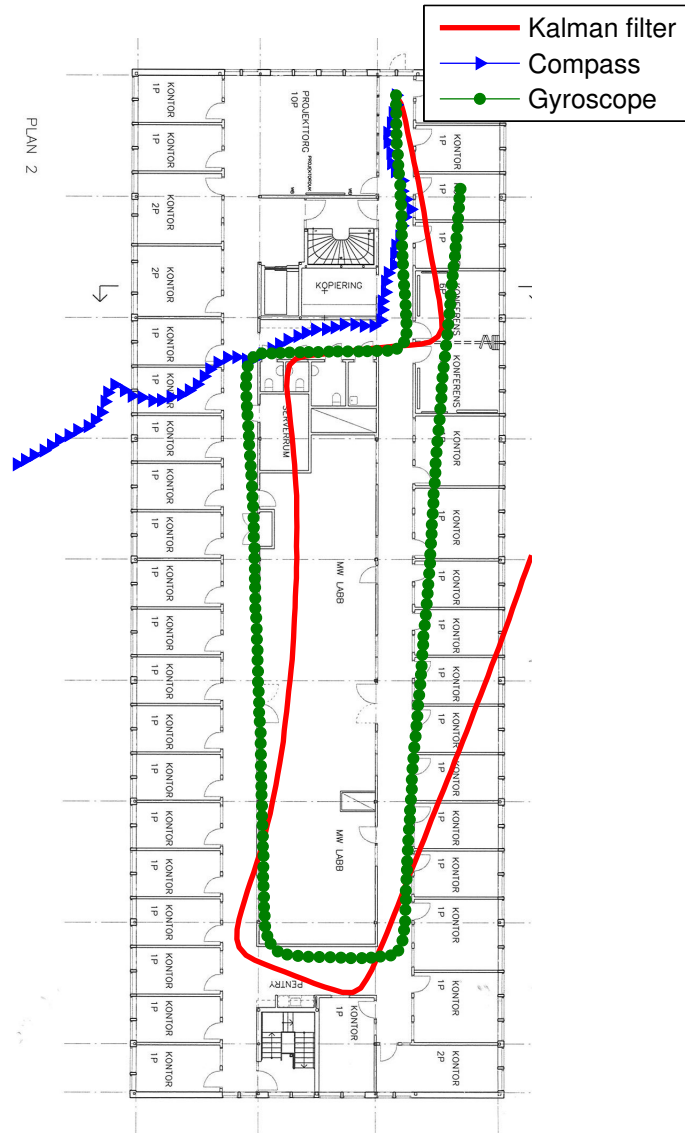**Figure 4.12:** Trajectory affected by movement.

Figure 4.13: Undetected disturbances affect the Kalman filter performance.

Chapter 5

Conclusion

T HE PURPOSE of this work was to find the position of a user on an indoor environment using only inertial and magnetic sensors on a mobile device. The motivation was to enhance existing tracking methods to locate people in risky environments. Different proposals to solve the distance and heading estimations were studied, and a simple sensor fusion algorithm was proposed to solve the positioning problem.

The overall results for the positioning system show an average error rate in position of less than 5% with only one test over this result. It is important to note that only one solution was used for all the experiments, meaning that no changes were made to the Kalman filter or disturbance detector for the different users and places. However, the scope of the project was limited to having the mobile device fixed in the waist or in the pocket of the user and enhancements must be done to adapt the system to situations were the phone is moving.

Further work must be done to recognize the location of the phone and to adapt the system accordingly. Location awareness algorithms have been designed for PNS applications, but they have not been applied to the complete tracking problem yet [14]. Algorithms to compensate for gait movements could be of help to reduce the impact on sensor data. Ongoing studies analyze the gait frequency depending on the position of the sensors which could help on this purpose [15]. Also, considering the map information and an adaptive step length algorithm could help to improve the overall performance of the system.

Bibliography

[1] M. Kayton, "Pacific northwest distinguished lecture - 100 years of inertial navigation", *Aerospace and Electronic Systems Magazine,* IEEE, Issue 9, 2008.

[2] J. Käppi, J. Syrjärinne, J. Saarinen, "MEMS-IMU based pedestrian navigator for handheld devices," in *Proc. of ION GPS*, Salt Lake City, UT, USA, 2001.

[3] *Using the ADXL202 in Pedometer and Personal Navigation Applications*, Application Notes AN-602, Analog Devices, [Online]. Available: `http://www.analog.com/static/imported-files/application_notes/513772624AN602.pdf`

[4] L. Fang, P. J. Montestruque, L. A. McMickell, et. al., "Design of a wireless assisted pedestrian dead reckoning system - the NavMote experience," *Instrumentation and Measurement*, IEEE Trans. Vol 54, Issue 6, 2005.

[5] S. H. Shin, C. G. Park, J. W. Kim, et. al., "Adaptive step length estimation algorithm using low-cost MEMS inertial sensors," *IEEE Sens. Applications Symposium*, San Diego, CA., 2007

[6] W. Chen, R. Chen, Y. Chen, et. al., "An effective pedestrian dead reckoning algorithm using a unified heading error model," *Position, Location and Navigation Symposium*, IEEE/ION, 2010.

[7] Q. Laddeto, J. van Seeters, S. Sokolowski, et. al., "Digital magnetic compass and gyroscope for dismounted soldier position and navigation," in *Proc. NATO-RTO Meetings*, Istambul, Turkey, 2002.

[8] M. J. Caruso, "Applications of magnetoresistive sensors in navigation systems," *Sens. Actuatiors*, pp. 15-21, 1997.

[9] J. W. Kim, H. J. Jang,D. H. Hwang, et. al., "A step, Stride and Heading Determination for the Pedestrian Navigation System," in *Journal of Global Positioning*, Vol 3, Issue 1, pp. 273-279, 2005.

[10] G.Welch, G.Bishop, *An Introduction to the Kalman filter,* University of North Carolina at Chapel Hill, Chapel Hill, NC 27599-3175, pp.19-29, 2001.

[11] E. Foxlin, "Inertial heading-tracker sensor fusion by a complementary separate-bias Kalman filter," in *Proceeding of VRAIS* IEEE, 1996.

[12] R. Jirawimut, P. Ptasinski, V. Garaj, et. al., "A method for dead reckoning parameter correction in pedestrian navigation," *Instrumentation and Measurement*, IEEE Trans. Vol 52, Issue 1, 2003.

[13] R. G. Brown, P. Y. C. Hwang, Introduction to Random Signals and Applied Kalman Filtering, 3rd ed., John Wiley & Sons, Inc., 1997.

[14] S. H. Shin, M. S. Lee, C. G. Park, "Pedestrian Dead Reckoning System with Phone Location Awareness Algorithm," *Position, Location and Navigation Symposium*, IEEE/ION, 2010.

[15] R. Takeda, S. Tadano, M. Todoh, et. al., "Gait analysis using gravitational acceleration measured by wearable sensors," *Journal of Biomechanics*, Vol 42, 2010.

[16] *iNEMO: iNErtial MOdule V2 demonstration board based on MEMS sensors and the STM32F103RE*, ST Microelectronics. [Online]. Available: `http://www.st.com/internet/evalboard/product/250367.jsp`

[17] *MATLAB*, MathWorks. [Online]. Available: `http://www.mathworks.com/products/matlab/`

[18] *Google Maps*, Google. [Online]. Available: `http://maps.google.com/`